Formation of graphene and hexagonal boron nitride on Rh(111) studied by in-situ scanning tunneling microscopy

Dong, G.

Chapter 1 Introduction

In this thesis, the formation of hexagonal boron nitride (*h*-BN) 'nanomesh' structures and of graphene on Rhodium (111) is studied experimentally. The structures of *h*-BN and graphene are extremely similar: both of them are single atomic layers with a honeycomb lattice, and the lattice constants are nearly identical. Both materials introduce novel properties and have the potential for a variety of applications. In this thesis, the layers were grown by chemical vapor deposition (CVD) on Rh(111). During growth, the formation processes were tracked by scanning tunneling microscopy (STM). This was performed *in situ*, namely during deposition at the elevated temperatures, required for the growth. In this way, we have obtained detailed knowledge of the formation mechanisms. In this thesis, basic surface science principles are employed to explain the observed, special growth behavior. Our understanding of the mechanisms at play has enabled us to compose new, improved deposition recipes that result in higher quality nanomesh and graphene layers. This knowledge is not only valuable for these specific systems, but it also deepens our general insights into deposition and growth of atomically thin layers.

1.1 Ultrathin film deposition

The deposition and growth of thin films on well-defined substrates forms one of the traditional topic areas of surface science [1-5]. The idea usually is to use the film to modify the surface properties, either chemically, electronically, optically, mechanically, etc. The deposited films are often base materials for practical applications, such as electronic devices, protective coatings, anti-reflection coatings, and coatings to reduce friction and wear. The importance of applications in each of these directions has been a real thrust for the surface-science investigations of the laws that govern the nucleation and the growth, the structures that form, the preferred orientations, the interfacial

arrangements, including mixing layers and misfit dislocations, the larger-scale grain structure, the smoothness or roughness, the strain in the film, etc. Nowadays, a dominant role is played by the nucleation and growth of single- or few-monolayer films that form in a self-limiting fashion that automatically leads to the formation of the thinnest possible films. These films may be either regarded as an interesting coating of the underlying materials, as a scaffold for further deposits, or as a thin foil that is to be detached later from the substrate on which it is grown, in order to be transferred to either another substrate or to a suspension structure for application as a free-standing film. The two materials that this thesis concentrates on are *h*-BN nanomesh [6] and graphene [7, 8].

1.2 Nanomesh

The spontaneous formation of a regular superstructure of hexagonal boron nitride (*h*-BN) on a metal surface was first reported by Corso et.al in 2004 [6]. The original recipe for preparing the overlayer is the exposure of a Rh(111) surface at 1050K to a low pressure of pure borazine gas $(HBNH)_3$. The *h*-BN layer that results from this procedure was found to adopt a highly regular superstructure that has been called the 'nanomesh', with 2 nm diameter depressions and a 3.2 nm period, as observed by scanning tunneling microscopy (STM). An example of an STM image of the nanomesh structure on Rh(111) is shown in Fig. 1.1.

1.2.1 The structure and properties of nanomesh

Ultraviolet photoelectron spectroscopy (UPS) revealed a splitting of the σ-band, which indicated two different types of bonds between the overlayer and the Rh [6]. Based on these observations, the atomic structure proposed by the first report was two atomic layers of hexagonal boron nitride, with holes in each layer. This was regarded as an ideal self-assembling template, since the dangling bonds at the edges of the holes in the top layer would be available as a regular pattern of binding sites for other molecules, with a

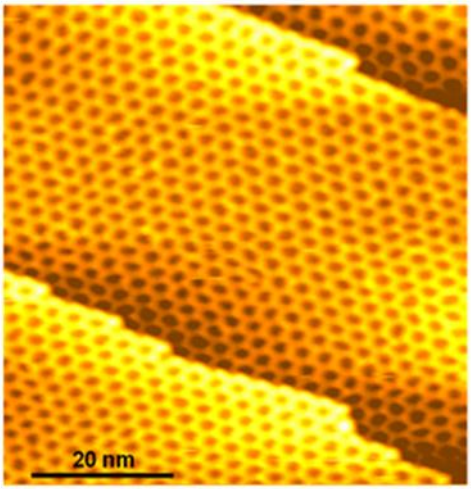

Fig. 1.1 An STM image of the *h*-BN nanomesh structure, prepared by exposing a Rh(111) surface to borazine at 1050K. (part I of this thesis) The structure features 2 nm diameter holes and a period of 3.2 nm.
Sample voltage: V_b = 1.4 V. Tunneling current I_t = 0.05 nA.

wide variety of possible functionalities. However, subsequent theoretical calculations showed that the two-layer model costs too much energy, and that the most probable model structure is one consisting of a highly corrugated single *h*-BN layer [9-11]. The single-layer model was soon confirmed by a surface X-ray diffraction (SXRD) study [12]. The size of the nanomesh unit cell is 13 x 13 BN units on 12 x 12 Rh atoms, which was reported by a low energy electron diffraction (LEED) study [6] and confirmed by theoretical calculations [9-11], SXRD [12, 13], and high-resolution STM [14]. Recently, a LEED study of *h*-BN formation on Rh-(yttria-stabilized zirconia)-Si(111) exhibited a (14 x 14) BN on 13 x 13 Rh(111) superstructure [15]. The reason for this is still under debate [13]. High-resolution SXRD showed that the 13 x 13 BN on 12 x 12 Rh structure is stable up to a temperature of 1107 K. From this collection of studies, we can conclude that the structure of the *h*-BN nanomesh on bulk Rh(111) is a single, corrugated layer of *h*-BN, with hexagonally arranged high and low regions, which have a height difference of 0.55 Å [11]. The unit cell of the nanomesh pattern contains 13 × 13 unit cells of the *h*-BN lattice, fitting onto 12 × 12 unit cells of the underlying Rh(111) surface.

Although the nanomesh is a single-layer structure, it was demonstrated to be sufficiently corrugated to act as a two-dimensional scaffold for the deposition of bucky balls in the first report [6]. Further studies showed that it can be a template for assembling nanoparticles [16] and for trapping molecules [14, 17, 18]. The nanomesh coating has been demonstrated to remain intact under ambient conditions [12], in liquids [19], and at high temperatures [13, 20], thus protecting the underlying metal. This stability makes the nanomesh an ideal template and coating with great application potential.

1.2.2 *h*-BN growth on other metals

h-BN can be grown as a single-layer structure on many metals [9, 11, 16, 21-29], using the method of CVD. On most surfaces with a lattice constant that differs from that of the *h*-BN, a superstructure is found. Initially, all these superstructures were considered to be mere moiré patterns, i.e. straightforward beating patterns between the lattices. Interestingly, there are remarkable differences between the corrugation amplitudes of the superstructures on different substrates. For example, on Pt(111), the *h*-BN overlayer stays nearly flat [21, 30]. On the other hand, on Ru(0001), *h*-BN forms an extremely corrugated structure, similar to that on Rh(111), with a unit cell of 14 x 14 BN unit cells on 13 x 13 Ru unit cells [22, 28, 31, 32]. Studies using X-ray photoelectron spectroscopy (XPS) and SXRD showed the strength of the interfacial chemical interaction between *h*-BN and the substrates to rise in the series Pt(111)–Ir(111)–Rh(111)–Ru(0001) [21]. It was concluded that, in addition to the lattice mismatch, a large strength of interfacial chemical bonding is a prerequisite for the formation of a significantly corrugated layer [21, 30].

1.2.3 Formation mechanism of the nanomesh structure

In spite of the growing number of studies on the structure and properties of the nanomesh overlayers, the mechanisms by which these layers nucleate and grow are virtually unexplored [20]. This is due to several practical reasons. Firstly, the unit cell contains 13 x 13 BN units on 12 x 12 Rh atom distances, which is difficult for theoretical and computational approaches. Secondly, the conditions for the CVD reaction, in particular the required high temperatures, disqualify many experimental techniques, such

as STM. Thirdly, most of the methods that can be applied at high temperature only give information in reciprocal space and average over large surface areas, which makes it very difficult to extract the microscopic mechanisms at work. To reveal the details of the kinetic processes, local, real-space observations are more direct. One technique, which readily gives real-space images and can be used at elevated temperatures, is low-energy electron microscopy (LEEM). Unfortunately, the size of the nanomesh unit cell is just at the resolution limits of LEEM, so it is difficult to study the nanomesh growth in detail with that technique.

What are the influences of the high temperature and the superstructure on the growth of the nanomesh structure? The high temperature could be necessary to crack the borazine molecules, releasing hydrogen and possibly rupturing B-N bonds, in order to form reactive precursors that stick sufficiently strongly to the surface and serve as the growth units, from which the overlayer can be assembled. One can also imagine that a high temperature would be required to provide sufficient lateral mobility for crystallizing the otherwise disordered overlayer into the perfectly periodic nanomesh structure. The growth unit of the nanomesh could be as simple as a single unit of *h*-BN, and the superstructure could just be formed as a moiré pattern. Or perhaps the superstructure also influences the growth process. To address these questions, a variable-temperature STM was used, which allows fast scanning and imaging over a wide range of temperatures and during substantial temperature changes [33, 34]. STM observations under the reported growth conditions, i.e. *during* borazine exposure at temperatures up to 1200 K, were carefully analyzed in this thesis, which unveiled the mechanisms of the adsorption, and the decomposition of borazine and the *h*-BN nucleation and growth in detail. These results are presented in part I of this thesis.

1.3 Graphene

Graphene is a planar sheet of sp^2-bonded carbon atoms, a single atom thick, which are densely packed into a honeycomb crystal lattice. Alternately, it can be viewed as a single atomic layer of graphite, while graphite itself consists of many graphene sheets stacked together. The interatomic distance of carbon atoms in graphene is 0.142 nm. Graphene is one of many carbon allotropes, along with diamond, graphite, carbon nanotubes, and

fullerenes. Diamond and graphite are three-dimensional (3-D) structures; carbon nanotubes can be considered a 1-D structure; fullerenes are molecules where carbon atoms are arranged spherically, and hence are 0-D objects; they feature discrete energy states [35]. Graphene fits nicely into the gap, being the 2-D allotrope of carbon. Among systems with only carbon atoms, graphene plays an important role**,** since it forms the basis for the understanding of the electronic properties of the other allotropes [35]. Besides its interesting and important physical properties, graphene also provides the focus for further application-oriented research, for example concerning its electronic performance (see next section) [35-37], in view of its possible role as a future replacement for silicon-based electronics. Because of its importance in the scientific world and for its applications, this simple material has drawn enormous attention during the last decade. Fig. 1.2 shows the recent increase of the publication rate of papers concerning graphene, especially after 2004, when the first experimental evidence was reported of the electronic properties of graphene [7, 38], and even more so after 2005, when follow-up experiments confirmed that its charge carriers were massless Dirac fermions [8, 39]. This lead to an explosion of articles devoted to graphene, which has been called the graphene 'gold rush' [38].

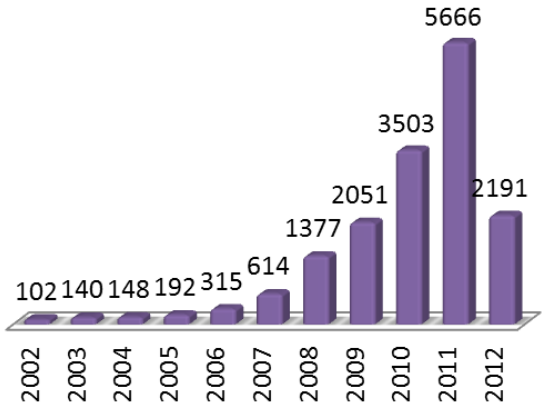

Fig. 1.2 The number of scientific papers published on graphene in each year over the last ten years. A dramatic increasing can be seen after 2005. This graph was obtained by searching the *ISI Web of Knowledge*^{TM} for the key word 'graphene' (including data up to May 3, 2012).

1.3.1 The properties of graphene

Graphene has many properties that make it special, for example, its electronic properties, its extreme mechanical deformability in combination with extreme yield strength, and its chemical stability in an atmospheric environment. The electronic properties of graphene are receiving most attention. They combine appealing fundamental physics with the potential for future electronics applications. Graphene can be considered as a basic building block for graphitic materials of all other dimensionalities. It can be wrapped up into 0-D fullerenes, rolled into 1-D nanotubes [40], or stacked into 3-D graphite [35, 38]. Theoretically, graphene (or '2-D graphite') has been studied for sixty years [38, 41, 42], and it has been used for describing properties of various carbon-based materials.

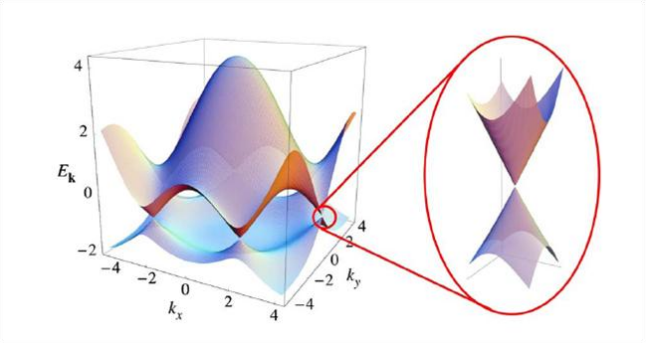

Fig. 1.3 Electronic energy dispersion of the graphene lattice. Left: the energy as a function of momentum components k_x and k_y in the plane of the graphene. Right: a zoom-in of the energy bands near one of the Dirac points. (From ref. [35])

In 2009, A.H. Castro Neto reviewed the basic theoretical aspects of graphene [35]. Graphene is a semi-metal, or zero-gap semiconductor, and has a linear dispersion at its Dirac points (Fig. 1.3). This was discovered by Wallace, using the tight-binding approximation, already in 1947 [41]. The energy dispersion for electrons in the vicinity of the Dirac points of graphene can be described by [35, 41]: $E_{\pm}(q) \approx \pm V_F|q| + O[(q/K)^2]$, where E is the energy with respect to the Fermi level, q is the difference in momentum from the Dirac point, and V_F is the Fermi velocity, with a value $V_F \approx 1 \times 10^6\, m/s$. This energy dispersion can be derived from the Dirac equation for massless particles. This behavior was demonstrated experimentally sixty years later [8, 39]. The Dirac electrons

can be controlled by the application of external electric and magnetic fields, or by altering sample geometry and/or topology [35].

Dirac fermions behave in unusual ways when magnetic fields are applied, which leads to special phenomena, such as the anomalous integer quantum Hall effect (IQHE) [8, 39] and the fractional quantum Hall effect (FQHE) [43]. Different from the IQHE observed in other systems, the IQHE in graphene can be observed at room temperature [35, 44]. In fact, the anomalous IQHE should be regarded as the trademark of Dirac fermion behavior. Another interesting feature of Dirac fermions is that they can be transmitted with probability unity through a classically forbidden region, due to the so-called Klein paradox [45].

1.3.2 Potential applications of graphene

The number of potential applications of graphene is enormous, and it seems to increase further every day. In order to provide an impression, I simply reproduce the list of proposed application areas of graphene that can be found on Wikipedia [46].

1. Room temperature distillation of ethanol for fuel and human consumption
2. Single-molecule gas detection
3. Graphene nanoribbons
4. Graphene transistors
5. Graphene optical modulators
6. Integrated circuits
7. Electrochromic devices
8. Transparent conducting electrodes
9. Reference material for characterizing electroconductive and transparent materials
10. Thermal management materials
11. Solar cells
12. Ultracapacitors
13. Engineered piezoelectricity
14. Graphene biodevices
15. Anti-bacterial
16. Study of liquids

Which of these applications will become truly dominant in its own application area remains to be seen. In any case it is evident from the long list and wide variety of potential practical applications that graphene should be expected to rapidly acquire significant economical and societal impact.

1.3.3 Graphene production

Graphene is a single layer of graphite, and graphite is a traditional base material, for example in lubricants, ink and pencils. So simply writing on paper with a pencil can create flakes of graphene. But the problem is that they cannot be located and distinguished easily from multilayer graphene or plain graphite (thick multilayers). The first experimentally produced and verified graphene was obtained in 2004 by mechanical exfoliation of graphite [7]. Scotch tape was used to repeatedly separate graphite crystals into progressively thinner pieces. The tape, with the optically transparent flakes attached to it, was dissolved in acetone and, after a few further steps, the flakes, including single-layer graphene, multilayer graphene and graphite, were transferred onto the native oxide on a Si wafer. Individual atomic planes were then 'hunted' for under an optical microscope. Later, researchers simplified the technique, and started using dry deposition, avoiding the stage where graphene floated in a liquid. Relatively large crystallites have been obtained by this technique. As remarked before, graphene is relatively easy to make, but hard to find. The key point of this method is the possibility of visual recognition of graphene on a properly chosen substrate, which provides a small, but noticeable, optical contrast under an ordinary optical microscope [7]. Most of the experiments on graphene have been performed using this method [43, 47]. It nicely provides experimentalists with the best quality in topographical flatness [47] and electron mobility [43]. With this method, electron mobility in graphene sample has reached 200,000 $cm^2 V^{-1}s^{-1}$ [43]. The drawback of this method is, of course, reproducibility. From an application point of view, it is hard to imagine any production facility using microscopes to find tiny bits of graphene for electronic devices.

Since 2004, researchers have tried out many ways for a reproducible, bottom-up production of graphene. One method is to heat silicon carbide to high temperatures (>1100 °C), in order to make it sublime silicon and thereby reduce its surface to graphene [48, 49]. The choice of the face of the silicon carbide that is used for graphene

creation, either silicon-terminated or carbon-terminated, strongly influences the thickness (i.e. the number of layers), mobility, and carrier density of the graphene. This process produces a graphene sample size that is dependent on the size of the SiC substrate. However, the size of the domains is still in the order of hundreds of nanometers [48, 49]. Although the QHE could be measured with the graphene samples created by this method [48], the electronic mobility in this graphene only reached 2700 $cm^2\ V^{-1}s^{-1}$, [50] which is much lower than for the scotch tape method.

1.3.4 Graphene growth on transition metals

A very promising alternative method to produce precisely one single layer of graphene is chemical vapor deposition (CVD) on transition metal (TM) surfaces [25, 51-58]. It is the method that we have concentrated on in the work described in this thesis. TMs are favorable substrates for graphene growth by CVD because they are excellent catalysts for hydrocarbon decomposition and they strongly bind the graphene that forms as a consequence, while newly arriving hydrocarbon molecules do not stick to or decompose on the graphene that has already formed. In addition, because the solubility of carbon in TMs often depends strongly on temperature, graphene can also be made using segregated carbon [51, 53, 57, 59, 60]. In most investigations of the growth of graphene, the graphene and its properties are typically inspected only after the growth, at room temperature or below. After samples have been prepared at high temperature and cooled down subsequently, it is not easy to distinguish which kind of carbon, segregated or deposited, has been responsible for the formation of the graphene layer. Actually, graphitic layers on TMs had been investigated much earlier [25-27, 59, 61, 62], before specific attention was paid to graphene.

As a consequence of its strong interaction with the substrate, graphene on top of TMs is very different from the idealized free-standing graphene. It does not have the interesting electronic properties mentioned before, but it does have its own special appeal, for example, being the template for the self assembly of additional overlayers [17], or the graphene-metal contact serving a spin filter [63, 64], etc. Recently, in order to produce free-standing graphene, several recipes have been introduced for transferring graphene from TMs onto other substrates [56, 60, 65, 66]. With these recipes, CVD-grown graphite layers on TMs have become a good candidate for producing high-quality graphene. A

promising carrier mobility of 4,000 to 7,350 cm^2 $V^{-1}s^{-1}$ has already been reported for graphene, obtained via this route [67-70]. The size of graphene made by CVD method is reported up to 30 inch [70].

No matter in what form the graphene is produced, free-standing or on a substrate, for many applications it is the structural quality of the graphene that limits its properties and therefore the quality of the final products in which it can be applied. The typical types of imperfections introduced by the CVD method on TMs are impurities and structural defects. The problem of impurities can be solved by using a sufficiently clean production setup and sufficiently clean materials (metal substrate and precursor gasses). The structural defects include other carbon phases (e.g. metal carbide), domain boundaries between different graphene patches, point defects [54] (e.g. pentagons and heptagons [71]) and thickness variations (voids or multilayers). It has been demonstrated that such defects can influence the electronic properties of graphene [71]. To reduce and eventually completely avoid the occurrence of structural defects, full control of the formation mechanism of graphene is necessary. This can only come through a thorough, atomic-scale understanding of the process. Once we have acquired a full understanding of the basic mechanisms of graphene formation and possible competing processes, we can use that to subsequently develop an optimal growth recipe.

In spite of their obvious importance, only a very limited number of experiments have directly addressed the important kinetic processes [51, 53]. CVD of graphene on TMs is typically performed at elevated temperatures, where the interaction between the carbon and the TMs can lead to very complex behavior. If measurements are performed at room temperature or lower, after the graphene has been grown, it is hard to infer the reaction path, especially if part of this path also involves the cool-down of the sample. Unfortunately, most of the experimental methods that can be used *in situ* at elevated temperatures do not have atomic resolution, which is also a prerequisite for obtaining detailed information on the growth kinetics [56].

Our special-purpose, variable-temperature scanning tunneling microscope (VT-STM) is well-suited for this purpose [33, 34], since it enables one to follow the reaction and growth of graphene *in situ*. Ethylene decomposition on Rh(111) is taken as a generic example of carbon deposition on TMs. The interaction between carbon and Rh can lead to carbide formation [72], carbon dissolution [73], and graphene formation [61]. These

are also the typical ‘products’ that can be formed on other TMs. Actually, carbon is the main contaminant in Rh crystals.

The complexity of the carbon-on-Rh(111) system makes it a good example for demonstrating, in general, the interaction between carbon and TMs. The 3-fold (111) orientation was chosen, to act as a template for graphene crystallization. In addition, graphene forms an easily recognizable moiré pattern on Rh(111). A simple calculation shows that the moiré pattern ‘magnifies’ the misfit defects between the lattice of the graphene layer and that of the Rh substrate. For example, 1 degree of actual graphene rotation with respect to the Rh lattice results in a 10 degree apparent rotation in the moiré pattern. In this way, atomic information about graphene can be achieved even without actually achieving atomic resolution in STM. In part II, detailed observations of this system are provided, such as the temperature range for graphene and carbide formation and for their stability, the dependence of the forming structures on temperature, and the role of the precise initial conditions. Armed with this information, we demonstrate that a higher-quality graphene can be obtained. Also carbide formation can be avoided, and the dissolved carbon can be controlled to form graphene. Based on this, we attempt to derive the optimal recipe for obtaining low-stress, single-orientation, single-crystalline, single-layer graphene.

1.4 This thesis

This thesis starts with a detailed description of the experimental setup and basic experimental procedures in Chapter 2. The main component of the thesis is devoted to the formation of monolayers on Rh(111). This is organized in two parts, part I (from Chapter 3 to Chapter 6) concerning the growth of *h*-BN nanomesh overlayers and part II (from Chapter 7 to Chapter 13) to the growth of graphene. Each part starts with a short introductory chapter (Chapter 3 and Chapter 7). The thesis ends with a summary for the layman.